ELSEVIER

Cement & Concrete Composites 25 (2003) 787–799

Cement & Concrete Composites

www.elsevier.com/locate/cemconcomp

Modal testing and dynamic FE model correlation and updating of a prototype high-strength concrete floor

A. Pavic *, P. Reynolds

Department of Civil and Structural Engineering, University of Sheffield, Sir Frederick Mappin Building, Sheffield, Yorkshire S1 3JD, UK

Received 24 January 2002; accepted 27 August 2002

Abstract

This paper presents results of modal testing of a unique full-scale 15 × 15 m floor structure made of in situ cast high-strength concrete (HSC) having strength of at least 115 MPa. In addition, finite element (FE) modelling of this floor, model correlation with experimental results and subsequent 'manual' model updating to match correlated pairs of natural frequencies and mode shapes are described. As the concrete floor was tested and updated for both uncracked and uncracked states, the FE model updating provided a valuable insight in the change of floor stiffness between the uncracked and cracked states. It was found that even a heavily cracked HSC floor remains linear and does not have significantly increased damping under low-level excitation. Also, bending of in situ cast HSC columns provided considerable stiffness to the floor even when heavily and visibly cracked. Finally, FE model updating confirmed that dynamic modulus of elasticity of the as-built HSC was about 47 GPa and, therefore, considerably increased compared with normal strength concrete.

Keywords: High-strength concrete; Cracking; Forced vibration; Modal testing; Vibration serviceability; Modal analysis; Finite element model correlation; Updating

1. Introduction

A concrete floor is an integral part of practically every modern industrial, commercial or residential building. Modern suspended concrete floor structures are becoming increasingly bold in conception and slender in cross section. To achieve this, relatively new construction techniques and new quality construction materials, such as cast in situ high-strength concrete (HSC), are gaining popularity. As floor slenderness increases, so does the possibility of problems with vibration serviceability of such floors under footfall or other types of relevant dynamic loading in buildings. However, currently little is known about vibration performance of as-built full-scale slender concrete floors made of HSC having strength of 100 MPa or more.

This paper presents results of a combined analytical and experimental investigation into modal properties of a unique full-scale prototype HSC floor before and after considerable deflection and serviceability cracking occurred in it. The test structure was an experimental slab designed as a part of a BRITE EURAM demonstration project on feasibility of in situ HSC funded by the European Union. The floor was the strongest full-scale concrete slab ever produced in Europe [17]. The slab was cast indoors on 10 October 1995 in a large workshop at Taywood Engineering in West London (Fig. 1). Its decommissioning took place in June 1998. The writers seized a unique opportunity, given by Taywood Engineering and Ove Arup & Partners, the latter being the principal designers of the floor, to test dynamically this exceptional structure.

2. Description of floor structure

The floor was a 15 m symmetric 250 mm thick square plate, being directly supported by four 300 × 300 mm columns. The columns were 1.6 m high and set in 3.0 m from the floor edges (Fig. 2). They were founded on 400 mm deep and 2.0 m square footings, which, in turn, were supported by the workshop's strong floor. The slab

* Corresponding author. Tel.: +44-144-222-5721; fax: +44-144-222-5700.

E-mail address: a.pavic@sheffield.ac.uk (A. Pavic).

0958-9465/$ - see front matter © 2002 Elsevier Ltd. All rights reserved.
doi:10.1016/S0958-9465(02)00100-2

Fig. 1. Reinforcement placement and casting of columns prior to slab concreting (courtesy of Taywood Engineering Ltd.).

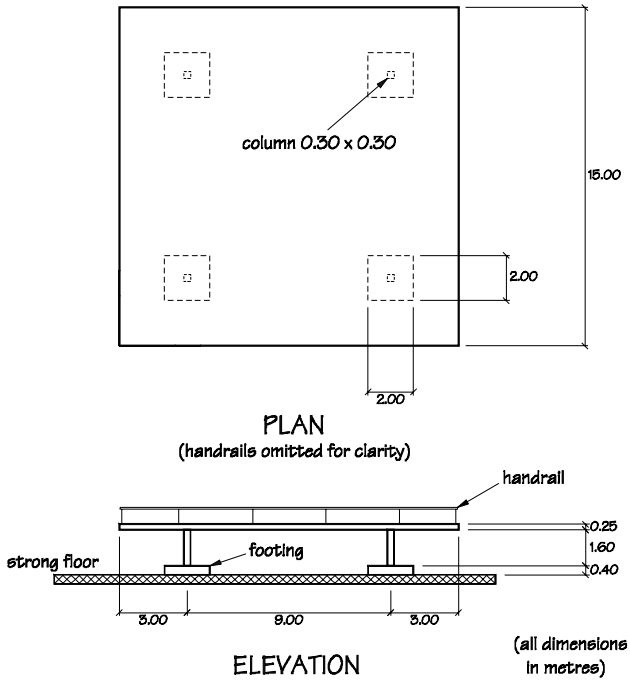

Fig. 2. Layout of classically reinforced in situ cast HSC floor.

boundary conditions along the edges of the 3.0 m cantilevers were completely free. Also, 1.0 m high safety handrails were clamped approximately every 3.0 m along all four edges (Fig. 2). The slab was classically reinforced with two layers of meshed unstressed reinforcement placed in the bottom and/or top zones of the slab depth, as appropriate (Fig. 1). Further details about this structure are presented by Price [17].

Spanning 9.0 m between the columns, the slab's span-to-depth ratio was 36, which can be considered to be extremely slender for a classically reinforced concrete floor [3].

3. Field test(s) planning

As a part of an EU funded research project, which was completely separate from the research reported in this paper, the floor had to be loaded twice and its serviceability performance examined in terms of deflections and cracking. Firstly, only three days after casting, the slab was loaded to 1.5 kN/m^2 plus dead weight. Then, 28 days after casting, it was loaded to 13.125 kN/m^2 including dead load [17]. The loading was applied by a system of 36 hydraulic jacks and pre-stressing bars, which passed through the slab and were anchored in a strong floor underneath (Fig. 3). The first load was considered to be light and was meant only to cause deflections with no cracking of the slab. However, the second, much increased, load was aimed at causing extensive deformation and cracking. Both loading conditions were, nevertheless, within the design serviceability loading limits [17] meaning that no failure of the slab was expected.

In the context of this two-phase static testing, it was interesting to compare the floor's vibration performance at the following three distinctive stages in the life of this structure:

- Stage 1: immediately after the slab was cast;
- Stage 2: between the light and the heavy loading; and
- Stage 3: after the heavy loading.

3.1. Test methodology

The main aim of the dynamic testing was to measure floor modal properties: natural frequencies, mode shapes and modal damping ratios. In principle, when performing structural modal testing it is advisable to measure both the excitation and the corresponding response, leading to frequency response functions (FRFs) [6]. Methodologies based on response-only measure-

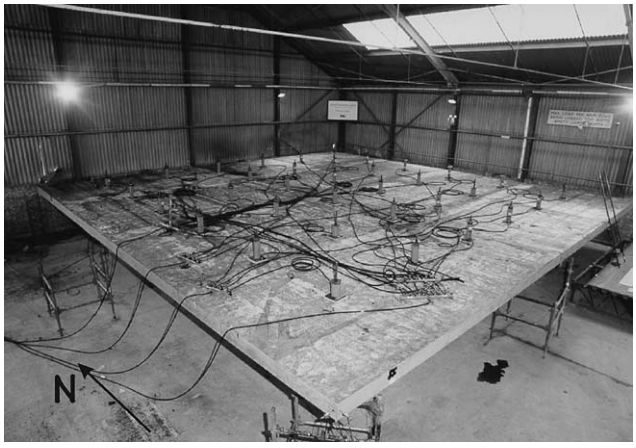

Fig. 3. Static loading test setup (courtesy of Taywood Engineering Ltd.).

ments, such as heel-drop excitation or ambient vibration survey, typically do not produce sufficient amount of information necessary to perform accurate enough experimental modal analysis of a structure with closely spaced modes of vibration. These are typically developed in real-life floor structures, such as the test floor, which have numerous symmetries and/or repetitive geometry.

When performing FRF measurements on building floors either impact or shaker excitation is used in practice nowadays. In this testing the floor was impacted manually by a sledge hammer, the operator of which was sitting in a chair and trying to be very still during data capture after the impact (Fig. 4). The data from one hammer and one accelerometer channels were digitised and further processed in situ using Diagnostic Instruments DI2200 portable digital spectrum analyser.

The DI2200 spectrum analyser can apply an exponential window function $w_{\exp}(t)$ to both input and output channels. In this particular instrument the windowing function is defined by specifying the TC constant in the following formula:

$$w_{\exp}(t) = \exp\left\{ -\left(\frac{\mathrm{TC}}{T_{\mathrm{acq}}}\right) t \right\} \tag{1}$$

where T_{acq} is the data acquisition time, and t is time. The value of TC can be an integer between 0 (no exponential windowing) and 10. The greater TC, greater the exponential decay. Theoretically speaking, the only consequence of the application of the exponential windowing in the hammer modal testing is an (artificial) increase of modal damping ratios in the measured FRFs [11]. This was necessary in order to increase the number of FRF data points within the half-power bandwidth to 5 or more, as recommended by the UK Dynamic Testing Agency to ensure good quality FRF curve-fitting [4]. However, it should be said that it is possible to recover the real damping ζ_r afterwards by applying the following formula [11]:

$$\zeta_r = \zeta_{r,\mathrm{windowed}} - \frac{\mathrm{TC}}{T_{\mathrm{acq}}} \frac{1}{2\pi f_r} \tag{2}$$

where $\zeta_{r,\mathrm{windowed}}$ is the modal damping ratio for the rth mode of vibration estimated from the 'windowed' FRFs.

Fig. 4. Hammer excitation and data acquisition.

3.2. Special circumstances

Severe time constraints of only 24 h per test played an important role in the planning of the dynamic testing, as is usually the case when performing dynamic testing of full-scale civil engineering structures in field conditions.

For example, as there were only three days between the slab casting and the application of the first loading, it was not feasible to carry out Stage 1 dynamic testing. Therefore, only the remaining two stages were possible to be investigated. Also, although the slab was located indoors, the testing conditions were not up to normal laboratory standards as no heating existed and the workshop itself was very noisy due to other activities. The worst example of this was the running of an aircraft engine only 50 m away from the place where the slab was erected. While the engine was running no dynamic testing of the floor was possible. Also, other frequent sources of extraneous noise had the potential to affect the quality of experimental data.

3.3. Site visit

One site visit prior to even preliminary field modal testing is recommended [5] in order to gain familiarity with the test structure and its environment. This is fully supported by the writers' experience in that up to half of the total site time can actually be devoted to activities such as accessing the structure, the equipment (un)packing, (dis)connecting, setting-up, checking and trouble-shooting. Familiarity with the test structure, its site and environment can reduce uncertainties associated with these time consuming activities, and this is very important if the test is to be completed during the allotted time period.

Also, when using hammer excitation on floors, the first site visit can be used, if possible, to do some quick FRF measurements in order to ascertain whether additional floor 'de-rattling' procedures are necessary. It is well known that hammer impact testing is particularly sensitive to rattling of the structure being hit [8]. Floors usually have non-structural elements attached which may rattle, introducing non-linearities and thus giving poor test results.

The HSC floor site was visited for a brief period of only 4 h and a number of quick FRF reciprocity and homogeneity checks were performed by a two-strong test crew using the sledge hammer as the exciter. Although

the pre-stressing bars were removed, it appeared that the presence of 36 hydraulic jacks loosely positioned on the top surface of the floor (Fig. 3) caused the structure to fail an FRF reciprocity check. Problems were experienced with the homogeneity checks as well [4,5]. Hence, a 'de-rattling' procedure, in the form of stripping the floor surface of everything 'non-structural', apart from the safety handrails (required by safety regulations), was suggested and carried out. The first site visit was also used to check the essential geometric properties of the structure being tested and the levels of excitation due to background noise which were found to be considerable, but removable by using an H_1 estimator and FRF averaging [14].

3.4. Pre-test analysis

Finite element (FE) modelling and theoretical modal analysis were performed using the ANSYS code and, in particular, BEAM4 and SHELL63 elements from its extensive library [1]. The FE model developed in the pre-test analysis utilised SHELL63 elements to represent the HSC flat plate. As no cracks were anticipated in the slab, isotropic properties were assumed for this element. Following the spirit of a number of floor vibration serviceability guidelines, including those given by the Concrete Society [3], the relatively thin 300×300 mm columns (Fig. 2) were modelled as pin-supports.

The pre-test analysis FE model was relatively crude. It consisted of $6 \times 6 = 36$ elements having a uniform thickness of 250 mm, and nodes positioned to match the adopted experimental test-grid of 49 points shown in Fig. 5.

Values of the dynamic modulus of elasticity and density of the HSC used in the pre-test analysis were based on ultrasonic pulse velocity and concrete density measurements made by Taywood Engineering Ltd. The average ultrasonic pulse velocity through six HSC specimens made when the floor was cast was 4983 m/s, whereas the average material density was 2465 kg/m^3. The dynamic modulus of elasticity $E_{c,dyn}$ was then calculated using Eq. (3) [16], which links it with the ultrasonic pulse velocity V through concrete specimens having density ρ_c and Poisson's ratio v_c:

$$E_{c,dyn} = \frac{V^2 \rho_c (1 + v_c)(1 - 2v_c)}{(1 - v_c)} \quad (3)$$

For Poisson's ratio values increasing from 0.16 to 0.25 [16] the values of $E_{c,dyn}$ decrease from 57.5 to 51 GPa, respectively, when Eq. (3) is used. It should be stressed that the equation is applicable only to homogeneous, isotropic linear elastic materials [16]. These figures might appear high to a concrete designer used to operating with static elastic moduli in the range 20–30 GPa for normal concretes.

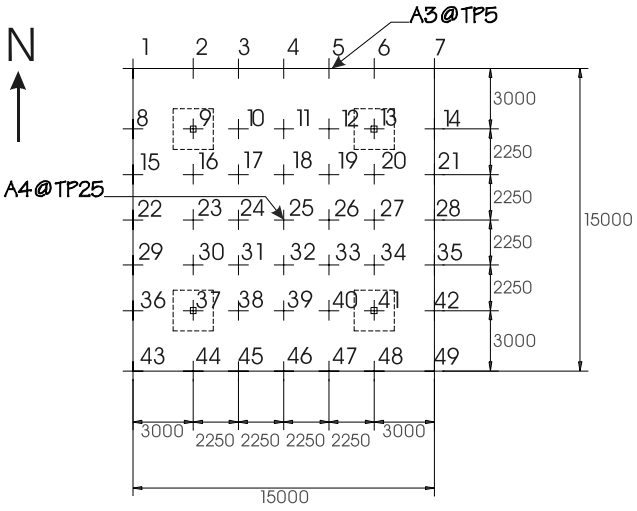

Fig. 5. Test grid and accelerometer locations.

However, Lyndon and Iacovou [12] reported that HSC can have a significantly increased dynamic modulus of elasticity when compared with the values obtained from normal strength concrete. The HSC considered here was designed to have strength of 110 MPa after 28 days (i.e. to be concrete grade C110). In fact, only three weeks after the casting, when the first dynamic testing took place, its strength was already at 115 MPa [17]. Given these considerations, it was decided to adopt $E_{c,dyn} = 50$ GPa in the pre-test analysis.

The initially calculated natural frequencies are shown in Fig. 6 and are summarised in Table 1. The Auto-MAC matrix calculations based on the pre-test FE model indicated that the test grid was likely to be suitable for the prevention of spatial aliasing [15].

3.5. Instrumentation, excitation and data collection

The dual-channel testing facilities for this test are shown in Fig. 4. The calculated natural frequencies (Table 1) indicated that repeated or closely spaced modes of vibration may occur in the real structure. This required a careful selection of the FRF reference point(s) which would be able to identify all relevant lower modes of vibration, which are excitable by, say, normal walking and therefore of interest when checking vibration performance and serviceability of this structure.

By inspecting the first four calculated modes (Fig. 6), modes 1 and 2 can be considered as relatively close, whereas modes 3 and 4 are repeated. In this particular case, when selecting the FRF reference point, the full value and importance of a pre-test analysis can be demonstrated quite effectively.

Typically, without performing any FE analysis and by exercising engineering judgement, an obvious choice for a reference point to measure the first mode of vi-

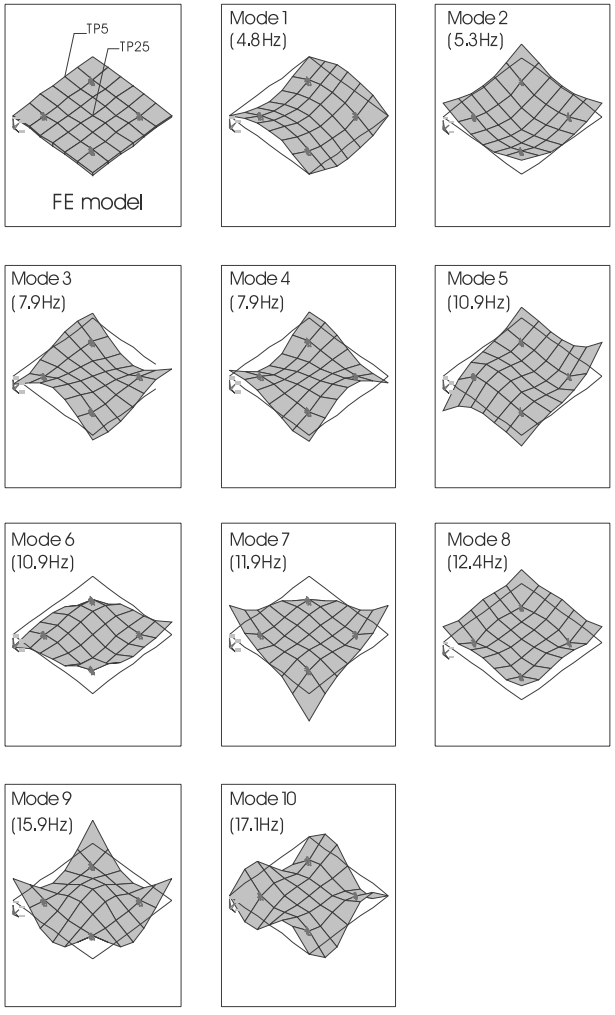

Fig. 6. Results of pre-test FE modal analysis.

Table 1
Natural frequencies calculated in pre-test FE modal analysis

Mode no.	Natural frequency (Hz)
1	4.8
2	5.3
3	7.9
4	7.9
5	10.9
6	10.9
7	11.9
8	12.4
9	15.9
10	17.1

bration would be TP25, the slab's mid-point (Fig. 5). However, the FE analysis clearly showed that the very same point could easily be a non-moving nodal point for modes 1, 3 and 4 (Fig. 6). Therefore, FRFs measured with the accelerometer at the slab's mid-point would, quite possibly, miss three out of the first four modes of vibration, including the very important fundamental mode.

Having this in mind, a decision was made to place the reference accelerometer at TP5, which appeared to move considerably in modes 1, 3 and 4 (Fig. 6), and to perform one hammer swipe over the 49 test points. Then, in order to comply with the requirement to measure more than one column/row of the FRF matrix [4,5], another hammer swipe was made with TP25 as the reference point. The main aim of second swipe was to ensure that the second mode of vibration was identified properly, as TP5 appeared to have a fairly small response in this mode (Fig. 6). Naturally, if more than two simultaneous data acquisition channels had been used, there would be no need to perform another time consuming and tiring hammer swipe.

4. Modal testing of the uncracked HSC slab at Stage 2

This modal testing consisted of preliminary investigation and FRF data acquisition and analysis.

4.1. Preliminary investigation

Initially a number of quick quality assurance (QA) measurements was performed. The main aim of these QA checks was twofold. Firstly, to select the digital data acquisition parameters for acquiring good quality FRF data (Table 2). Secondly, to establish the quality of FRF data that could be obtained from a notably quite noisy environment.

The acquisition parameters shown in Table 2 are those that were adopted when performing FRF measurements having TP5 as the reference. However, when TP25 was used as the reference, the principal aim was to identify only the second mode of vibration and, therefore, the frequency resolution was not the prime consideration. Therefore, instead of 0.05 Hz, the resolution for the second measurement was 0.1 Hz. As a consequence, the data acquisition times, number of data samples and frequency lines were halved for the same frequency range of interest. This was quite desirable considering the limited testing time and spectrum analyser internal memory available. However, the testing

Table 2
Main digital data acquisition parameters adopted for FRF measurements when TP5 is the reference point

Parameter description	Parameter value
Data acquisition time	20 s
Frequency resolution	0.05 Hz
Frequency range of interest	1–21 Hz
Total number of samples	1024
Number of frequency lines	400
Number of averages	5
Exponential window time constant (TC)	8

time constraints did not allow for more than five FRF averages.

4.2. FRF data acquisition and initial data analysis

Two FRF sweeps resulted in 98 FRFs which were acquired over 49 test points, half of these with TP5 as a reference, and half with TP25 as a reference.

The FRF data were generally noisy and there was a strong indication that the structure may have a number of close modes of vibration. Therefore, one of the mode indicator functions (MIFs), available in the ICATS [10] MDOF curve-fitting software, was used to pinpoint the frequencies which may correspond to the modes of vibration. This helps the selection of the frequency ranges of interest when performing either SDOF or MDOF single or multi-FRF parameter estimation exercises [9].

In this case, a very simple MIF, denoted as $|H_{j,\mathrm{sum}}(\omega)|$, and defined as the sum of the moduli of all measured FRFs, was selected. A mathematical expression of this MIF is:

$$|H_{j,\mathrm{sum}}(\omega)| = \sum_{k} |H_{jk}(\omega)| \tag{4}$$

Two MIFs were calculated. Firstly for the row of the FRF matrix corresponding to TP5 as the reference response point ($j = 5$), and, then, for the row where TP25 was the reference ($j = 25$). The calculated $|H_{5,\mathrm{sum}}(\omega)|$ and $|H_{25,\mathrm{sum}}(\omega)|$ MIFs are plotted in Fig. 7. The two curves integrate effectively information available in all the collected FRFs. The peaks in the two MIFs indicate the frequencies of the possible modes of vibration. By visually examining Fig. 8, it appeared that the two lowest modes of vibration could, indeed, be closely spaced (5.8 and 6.0 Hz). Other higher modes were clearly visible at 8.2, 14.8, 17.1 and 18.4 Hz. Finally there was a group of small peaks possibly indicating a number of closely spaced modes of vibration between 9.0 and 11.0 Hz.

Having established where to look for the modes of vibration, a number of parameter estimation exercises identified 12 modes between 1 and 21 Hz. Their properties are shown in Table 3.

By visually inspecting the FE calculated and experimentally estimated modes shapes (Figs. 6 and 8), the first three estimated modes resembled the FE modes 1, 2 and 4. Also, there was a clear correlation between analytical modes 9 and 10 and experimental modes 10 and 11, respectively. However, experimental modes 4–9 (shaded in Table 3) had much less consistent modal parameters than experimental modes 1–3, 10 and 11.

Finally, and most importantly, a notable difference was observed between the measured (Table 3) and analytically calculated (Table 1) natural frequencies for the first three correlated pairs of modes of vibration. Nevertheless, having in mind the very good correlation between the lowest three calculated and measured mode shapes, the writers were satisfied that modal data of

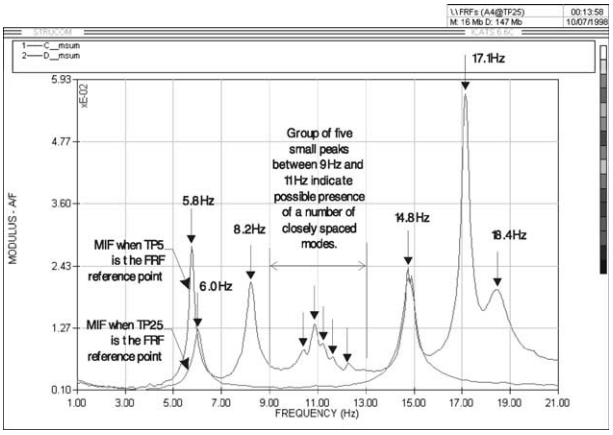

Fig. 7. Uncracked HSC slab—calculation of MIFs based on the summation of FRF moduli for two sets of 49 FRFs corresponding to TP5 and TP25, respectively.

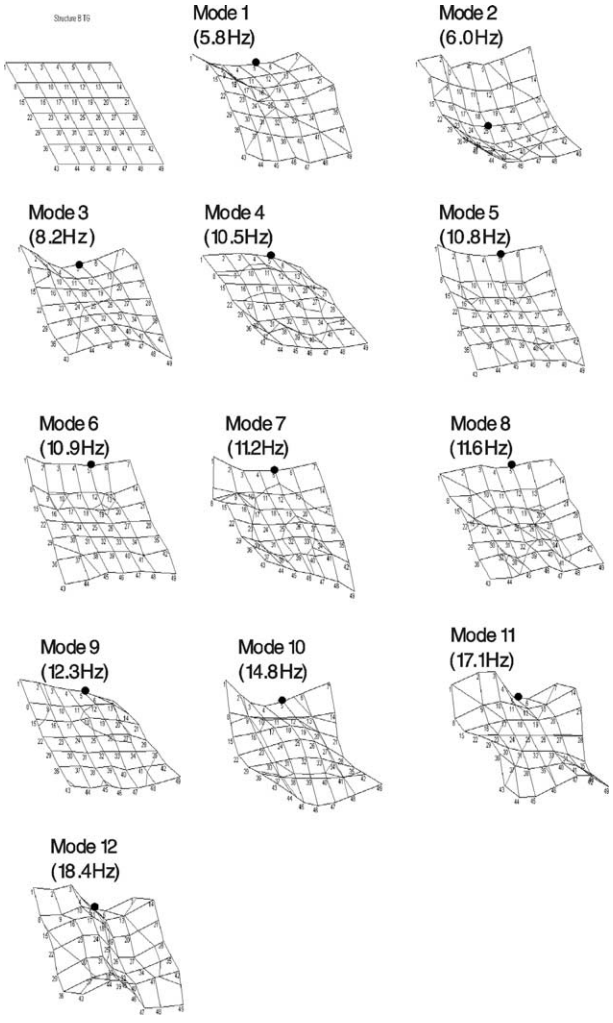

Fig. 8. Uncracked HSC slab—experimentally measured modes of vibration.

Table 3
Uncracked structure—the estimated natural frequencies and modal damping ratios

Mode no.	Frequency (Hz)	Modal damping ratio ζ (%)
1	5.8	0.51
2	6.0	0.54
3	8.2	1.19
4	10.5	1.12
5	10.8	1.00
6	10.9	1.65
7	11.2	0.36
8	11.6	0.23
9	12.3	0.30
10	14.8	0.73
11	17.1	0.39
12	18.4	2.08

Note: Highlighted are the analytical modes well correlated with the experimental data.

sufficient quality had been obtained. The differences, clearly indicating a lack of stiffness in the analytical model, could easily be attributed to inaccuracies in the relatively crude pre-test FE model. Further, more detailed correlation and updating exercises aimed at obtaining a more reliable analytical model of the structure are presented later in this paper.

5. Modal testing of the cracked HSC slab at Stage 3

As previously mentioned, the second round of testing of the HSC floor took place after the 13.5 kN/m^2 total static loading had been applied to the floor. This was achieved by 36 hydraulic jacks which were computer controlled in order to ensure as uniform as possible 'surface loading' across the whole area of the slab (including the cantilevers).

5.1. Cracking patterns

The 13.5 kN/m^2 loading caused extensive cracking in the floor, which remained visible even after the loading was removed. The crack patterns on the top and bottom surfaces of the slab were examined in detail and are shown in Fig. 9.

The writers' interpretation of the cracking patterns is that they conform to the way the reinforcement mesh was layered. As the top mesh had bars in the N–S direction lower than in the E–W direction, this made the N–S direction 'weaker' for the action of negative bending moments which put the top surface of the slab under tension. This tension opened a long E–W crack on the top surface (Fig. 9, top right). The bottom mesh also had N–S bars lower than E–W bars. However, for the action of positive bending moments, the E–W direction is now 'weaker'. This caused the cracks due to moments which bend the slab in this 'weaker' direction to be

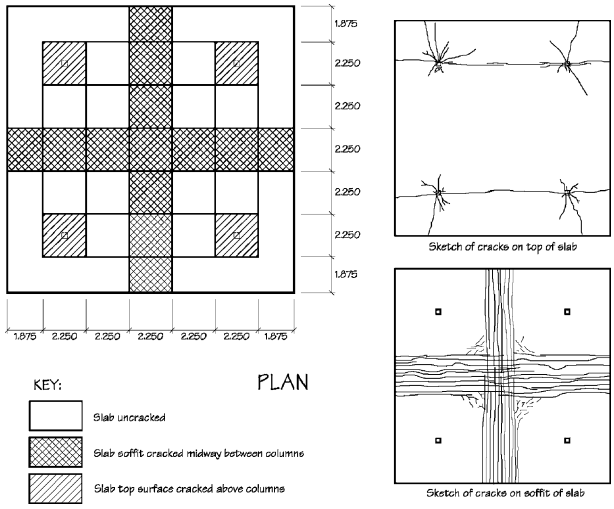

Fig. 9. Areas of slab used for modelling reduced stiffness due to cracking.

spread over a more narrow N–S strip (Fig. 9, bottom right).

The static loading caused extensive cracking at the top of all four columns as well (Fig. 10). The cracking propagation conformed to the state of biaxial bending, combined with an axial compression force, of the square 300 × 300 mm column cross sections.

5.2. Preliminary investigation

Having to investigate such a heavily cracked structure, the prime concern was its (non)linearity. A number of reciprocity and homogeneity FRF linearity checks was made. Considering the adverse environmental circumstances, the results were as good as for the same slab when it was uncracked. So, for the relatively low-levels of excitation and response, as would be expected in

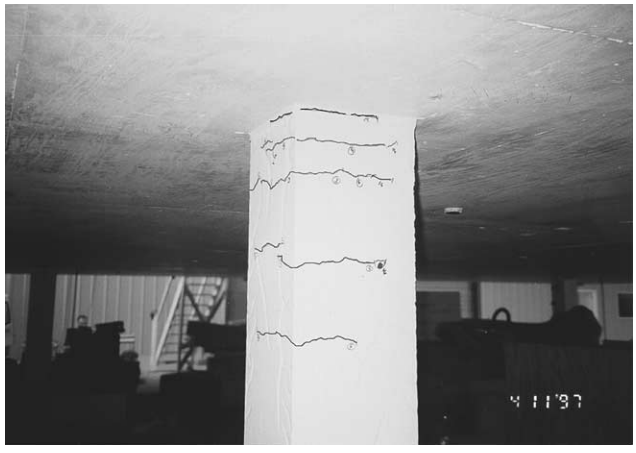

Fig. 10. Cracking pattern (enhanced for better visibility by a tracing pen) in column C2 looking from the North.

vibration serviceability checks, the structure could be considered as linear.

Regarding the digital data acquisition parameters selected for this second round of testing, the only changes to the values used in the first round (Table 2) was an increased number of averages from 5 to 10 and an increased exponential window time constant from TC = 8 to 10. More time available for testing allowed for more averages whereas the new time constant was the maximum which could be applied by the portable spectrum analyser. This was done in order to improve the signal-to-noise ratio during the 20 s of data acquisition per each hammer impact.

5.3. FRF data acquisition and initial data analysis

The same test grid comprising 49 points was used as for the first round of testing (Fig. 5). Two rows of 49 elements of the FRF matrix were measured by performing two separate hammer swipes using the same equipment as for the uncracked slab.

As it was anticipated that the cracking would change the stiffness distribution in the slab, and considering the results of the preliminary analysis, it was decided to use points TP5 and TP35 as the FRF reference points.

After the FRF swipes, two MIFs, $|H_{5,\mathrm{sum}}(\omega)|$ and $|H_{35,\mathrm{sum}}(\omega)|$, defined previously in Eq. (4), were calculated and their plots are shown in Fig. 11. As the lowest modes of vibration were of particular interest, the functions were visually examined and the lowest peak identified was at 5.0 Hz. However, a small 'bulge' on the left side of the peak at 5.0 Hz in $|H_{35,\mathrm{sum}}(\omega)|$ indicated the possibility that an even a lower mode of vibration existed.

To check this, another pair of MIFs, $\mathrm{Im}^2(H_{5,\mathrm{sum}}(\omega))$ and $\mathrm{Im}^2(H_{35,\mathrm{sum}}(\omega))$, being the summations of the squared imaginary parts of FRFs [10], was used. A mathematical expression of this new form of MIF, which is a readily available utility in the ICATS software, is:

$$\mathrm{Im}^2(H_{j,\mathrm{sum}}(\omega)) = \sum_k (\mathrm{Im}(H_{jk}(\omega)))^2 \tag{5}$$

where j is the FRF reference point. Two plots of this function corresponding to TP5 ($j = 5$) and TP35 ($j = 35$), as the reference points, were visually examined and another peak at 4.7 Hz became clearly visible, but only in $\mathrm{Im}^2(H_{35,\mathrm{sum}}(\omega))$ indicating that TP5 this time was not a particularly suitable reference point for measuring the fundamental mode of vibration.

After processing two rows of 49 FRFs and combining the results, 11 modes were identified. Their properties are shown in Fig. 12 and in Table 4.

The majority of modes was identified using TP35 as the reference point. The lowest two modes clearly show that the slab firstly bends in the less stiff E–W direction

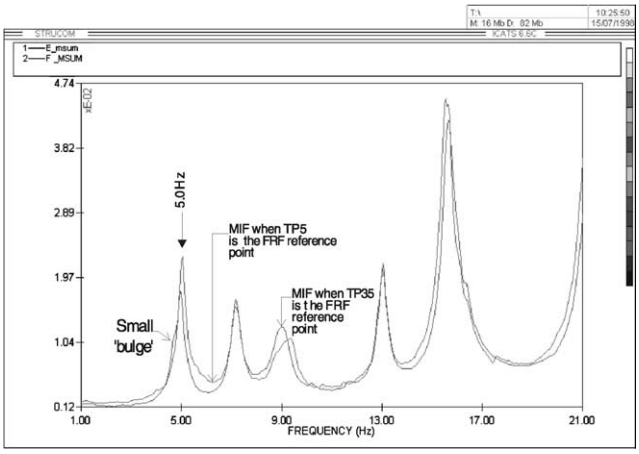

Fig. 11. Cracked HSC slab—two MIFs, being the summation of all measured FRF moduli in one row of FRF matrix, calculated for TP35 and TP5 as the FRF reference points.

and then in the stiffer N–S direction. This would be expected if the mode shapes were interpreted as the displacement configuration which minimises the potential and maximises the kinetic energy in each mode of vibration [15].

Although there was a number of peaks in the FRFs between 9.4 and 12.7 Hz, these failed to produce consistent modal estimates. An example of such uncertain estimates is mode 8 in Fig. 12 which has a peculiar mode shape and a very low damping value. This may indicate that this modal estimate is unrealistic. However, the shape of this mode resembled to some extent that of mode 9. This could indicate that mode 8 really existed, and was caused by the slight orthotropy in the slab developed by cracking. It was close to mode 9, but could not be estimated accurately using TP35 and TP5 as the reference points. Mode 9 is also interesting, as it was almost perfectly real whereas all of the other modes developed a certain degree of complexity [6] indicating possible presence of non-proportional damping.

6. FE model correlation and updating

The main aim of the FE model correlation and updating was to reconcile the analytical model with its experimental counterpart by matching as many as practicable pairs of analytical and experimental modes of vibration.

6.1. General procedure

Four methods for comparing the analytical and experimental modal properties, available in the ICATS suite of programmes, were used: (1) comparison of natural frequencies, (2) graphical comparison of mode shapes, (3) the modal assurance criterion (MAC) and (4)

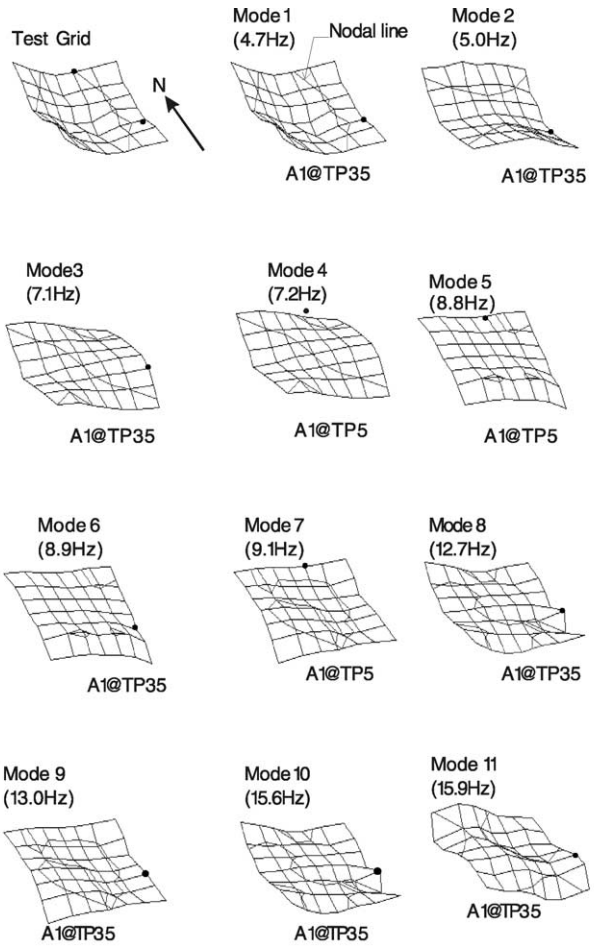

Fig. 12. Cracked HSC slab—the experimentally estimated mode shapes and natural frequencies. Black dots show which FRF reference point was used to identify the particular mode of vibration.

Table 4
Cracked structure—the estimated natural frequencies and modal damping ratios

Mode no.	Frequency (Hz)	Modal damping ratio ζ (%)
1	4.7	0.64
2	5.0	0.74
3	7.1	1.14
4	7.2	0.82
5	8.8	1.31
6	8.9	1.45
7	9.1	1.44
8	12.7	0.11
9	13.0	0.62
10	15.6	0.77
11	15.9	1.38

Note: Highlighted is the mode having unrealistically low damping ratio.

the co-ordinate modal assurance criterion (COMAC). These methods will be briefly outlined.

Firstly, the comparison of natural frequencies was done by tabulating and plotting of experimental (data Set 1) and analytical (data Set 2) natural frequencies (see top left graph in Fig. 13). This is simple but effective way of comparing the two sets of data. Secondly, graphical comparison of mode shapes was performed visually. Thirdly, the MAC matrix element corresponding to the ith experimental $\{\phi_X\}_i$ and jth analytical $\{\phi_A\}_j$ mode shape is defined as [13]:

$$\mathrm{MAC}(\{\phi_X\}_i,\{\phi_A\}_j)=\frac{|\{\phi_X\}_i^{\mathrm{T}}\{\phi_A^*\}_j|^2}{(\{\phi_X\}_i^{\mathrm{T}}\{\phi_A^*\}_j)(\{\phi_X\}_i^{\mathrm{T}}\{\phi_A^*\}_j)} \quad (6)$$

MAC matrix (Fig. 13, top right) values vary from 0 (0%) to 1 (100%) where the former indicates no correlation (i.e. mode shapes are linearly independent and their dot product is zero) and the latter indicates perfect correlation meaning that they are the same mode (i.e. one mode is a scaled version of the other which means that they are linearly dependent).

Whilst the MAC provides a good measure of global correlation between the mode shapes, when the correlation is not so good it fails to pinpoint geometrically the source of the error i.e. the DOFs generating the lack of correlation. Such a localisation of the error can be done by calculating the COMAC for each correlated DOF [13]. The number of COMAC values, typically, matches the number of experimentally measured DOFs. Each COMAC value, which ranges between 0 and 1, assesses the performance of the corresponding DOF averaged over the set of correlated mode pairs. The COMAC for ith DOF in the mode shape is defined as [13]:

$$\mathrm{COMAC}(i)=\frac{\left(\sum_{j=1}^{n_{\mathrm{CMP}}}|({}_A\phi_{ij})({}_X\phi_{ij})^*|\right)^2}{\left(\sum_{j=1}^{n_{\mathrm{CMP}}}|({}_A\phi_{ij})|^2\right)\left(\sum_{j=1}^{n_{\mathrm{CMP}}}|({}_X\phi_{ij})|^2\right)} \quad (7)$$

where n_{CMP} is the number of the correlated mode pairs. Lower values of the COMAC indicate poorer

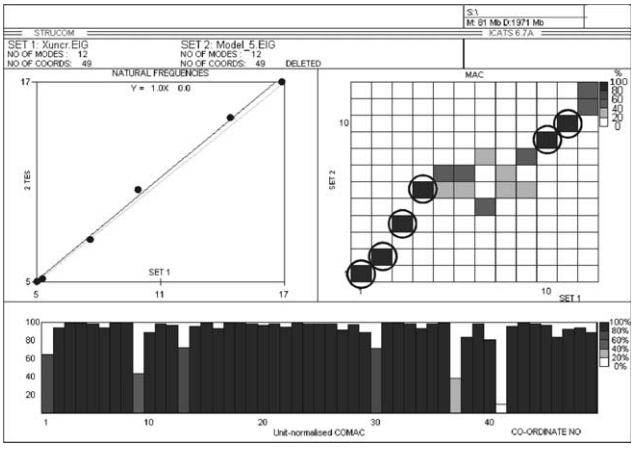

Fig. 13. Uncracked HSC slab—comparison of natural frequencies, MAC and COMAC.

performance of the particular DOF and possible errors either in its measurement or modelling.

FE model correlation and updating technology emerged in the 1990s as an indispensable design tool in mechanical and aerospace engineering and Friswell and Mottershead [7] wrote a comprehensive overview of it. Updating procedures are nowadays very much formalized and automated in various software packages. However, because of the complexity of open-space civil structures and poorer quality of experimental data, the application of FE model updating based on experimental measurements is still very much a research exercise in civil engineering dynamics. For example, Brownjohn and Xia [2] recently claimed that a representative but 'manually' updated (by trial and error) FE model must firstly be developed. Such a model should capture the main physical features of the real structure in a sufficient detail and be used as a starting point in the automatic updating. Such a model is then used in formalised sensitivity studies and automatic updating of a limited number of most uncertain modelling parameters, which is usually performed by a specialised software. Otherwise, updating software will struggle to produce a physically meaningful model converging to its measured counterpart. Therefore, the aim of the updating in this research was to demonstrate that a reasonable 'manually' updated FE model may be produced through a number of iterations informed by the four correlation methods mentioned above. Subsequent sensitivity studies and automatic updating were deemed to be beyond the scope of this paper.

6.2. Updating of uncracked slab structure

The aim of the manual updating of the uncracked slab structure was to match the lowest three measured modes of vibration with their analytical counterparts. The first FE model updating step, taken to address the observed lack of stiffness in the pre-test FE model, was to model the 300×300 mm columns.

The FE modelling was initially performed using a regular symmetric mesh of isotropic SHELL63 elements. The four columns, having 1.6 m clear height (Fig. 2), were modelled using four identical BEAM4 elements. The columns were assumed to be connected rigidly to the HSC slab and fully fixed at their bottoms. The main FE model tuning parameters were the length of the columns, assumed to be fully fixed at their bases, and the dynamic modulus of elasticity of concrete assumed to be the same in the slab and columns.

After a number of trial and error attempts, a length of 1.925 m of column system lines and a dynamic modulus of elasticity $E_{c,dyn} = 46.7$ GPa for the HSC produced analytical modes which correlated reasonably well with the selected three lowest measured modes of vibration. This is illustrated in Figs. 13 and 14. The MAC matrix in Fig. 13 shows that the third analytical mode shape (data Set 2) did not correlate with any of the measured modes (data Set 1), whereas the fourth analytical mode clearly corresponded to the third measured mode (Fig. 16).

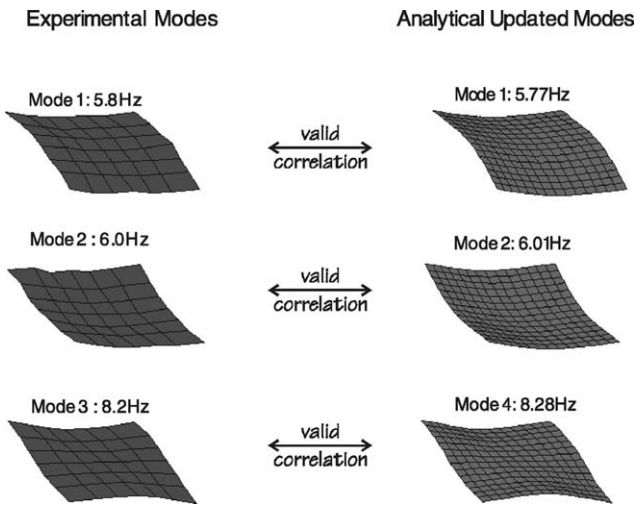

Fig. 14. Uncracked HSC slab—visual inspection of the first three pairs of correlated mode shapes.

This updating exercise showed that:

1. HSC can be expected to have a significantly increased dynamic modulus of elasticity compared to concretes of normal strength, and such increased values may be used in vibration serviceability calculations,
2. the in situ cast columns supporting uncracked in situ cast concrete floors can be expected to have a significant stiffening effect and should not be modelled as pin-supports, and
3. if the concrete floor of a flat plate configuration is uncracked, very reasonable FE modelling can be achieved by using isotropic shell elements, such as SHELL63 in ANSYS.

6.3. Updating of cracked slab structure

Considering the cracking patterns in the slab and columns (Figs. 9 and 10), FE model 2 was developed. The slab of this model consisted of four rectangular areas (Areas 1, 2, 3 and 4) and one square area around the columns (Area 5), as shown in Fig. 15. The dimensions of these areas and the orthotropic stiffness of the SHELL63 elements in the five areas could differ between the areas and could be changed parametrically during the updating. In addition, the cracked tops (25% of the height) of the four columns were modelled with BEAM4 elements whose bending stiffness could be changed parametrically and be different from that of the BEAM4 elements representing the lower uncracked portion of the columns.

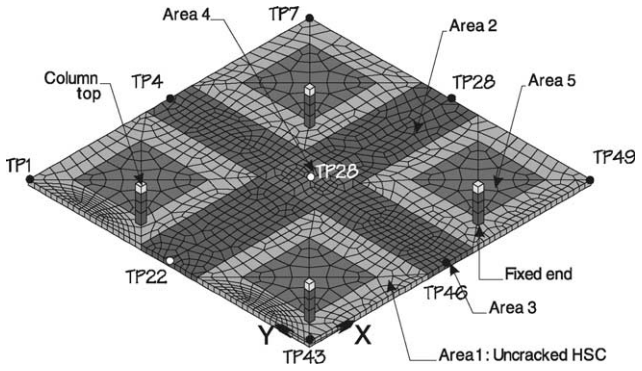

Fig. 15. Updated FE model of a cracked slab.

The main updating parameters used were:

1. the dimensions of the five cracked areas,
2. the five pairs of 'smeared' orthotropic bending stiffnesses corresponding to the five areas,
3. the dynamic modulus of elasticity for HSC, and
4. the bending stiffness of the cracked tops of the columns.

The results of the updating pertinent to the bending stiffnesses in the five areas are given in Table 5.

In addition, the updated dynamic modulus of elasticity was 47.5 GPa (increased from 46.7 GPa for uncracked model) and the cracked column bending stiffness was reduced to 78% of its uncracked stiffness. The last result indicates that even the visibly cracked HSC columns could be able to retain a significant portion of their uncracked stiffness for the level of excitation applied during the modal testing.

The updated FE model representing the cracked state of the structure is shown in Fig. 15. The lowest 10 natural frequencies calculated are presented in Table 6. However, it should be mentioned that exercises related to modelling of the cracked conditions proved to be much more difficult and time consuming compared to their counterpart for the uncracked case. As a consequence, it appears that the improved analytical FE model would have benefited from further updating, especially a refinement of distribution of stiffness in Areas 2 and 3. However, this would be difficult to do manually

Table 5
Cracked structure—updated parameters related to the properties of the five areas

Area	Rectangular area dimension in x direction (m)	Rectangular area dimension in y direction (m)	Percentage of 'uncracked' bending stiffness in x direction (%)	Percentage of 'uncracked' bending stiffness in y direction (%)
1[a]	n.a.	n.a.	100	100
2	12.6	3.0	100	58
3	2.4	12.0	40	100
4	2.4	3.0	40	75
5	3.6	3.6	90	35

[a] Area 1 is uncracked.

Table 6
Cracked structure—the analytically calculated natural frequencies and modal masses using the updated FE model

Mode	Natural frequency (Hz)
1	4.69
2	4.96
3	6.81
4	7.14
5	9.57
6	10.14
7	10.27
8	10.43
9	13.03
10	15.47

Note: Highlighted are the analytical modes well correlated with the experimental data.

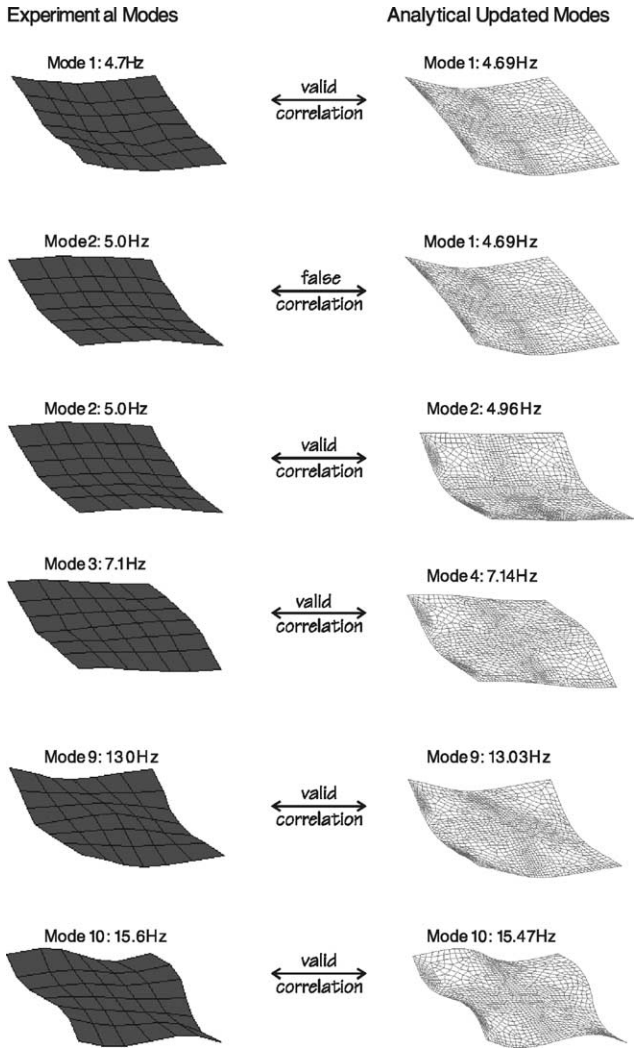

Fig. 16. Cracked HSC slab—the correlated experimental and analytical mode shapes.

and an automatic sensitivity study and updating procedure supported by appropriate software would be more efficient. This is, however, beyond the scope of this paper, as previously mentioned.

Nevertheless, a visual comparison of mode shapes (Fig. 16) shows that the manually updated FE model managed to capture the main features of the measured modes of vibration excitable by, say, walking at 4.7, 5.0 and 7.1 Hz. Also, it simulates remarkably well two higher measured modes at 13.0 and 15.6 Hz. All this increases the confidence in this 'manually' updated FE model.

7. Conclusions

Modal testing and 'manual' FE model updating of the full-scale prototype floor made of in situ cast HSC having enormous strength of at least 115 MPa proved that the bending stiffness of the supporting in situ cast columns made considerable contribution to the overall floor bending stiffness. As such, and contrary to widespread practice [3], even when heavily cracked, such columns should not be modelled as pin-supports when calculating floor modal properties for the purpose of vibration serviceability checks. Linear elastic FE models, where columns were modelled using bar elements rigidly connected to the floor and having their remote ends fully fixed, proved to be a fairly reliable means of calculating modal properties of in situ floors.

Also, extensive cracking of an HSC floor cast in situ reduced its natural frequencies considerably, compared with the uncracked condition. This was simulated successfully in the FE model by using orthotropic shell elements with reduced values of stiffness in the locations of the physical cracking, and in directions perpendicular to the main crack directions. Moreover, only a slight increase in the modal damping of the structure was observed as a result of cracking. Generally speaking, a modal damping ratio of about 1% for all modes excitable by normal walking seems to be a reasonable value, notwithstanding scatter present in the experimental data.

Furthermore, two 'manually' conducted FE model updating exercises confirmed that a significantly increased value of dynamic modulus of elasticity for in situ cast HSC floor. The value of about 47 GPa proved to be a reasonable assumption for both uncracked and cracked concrete having strength of at least 115 MPa.

Finally, advanced modal testing and 'manual' FE model correlation and updating technologies have been successfully transferred from the mechanical and aerospace engineering industries. The testing, correlation and updating procedures adopted and, in particular, the utilisation of MAC and COMAC proved to be invaluable in this research. It was demonstrated that the development of a relatively crude FE model prior to modal testing may be an important means of ensuring better quality of the experimental data. This is particularly so when the testing is performed under severe time constraints, as is likely to be the case for modal testing of large prototype civil engineering structures. Quiet conditions were shown to be essential for obtaining good quality results using instrumented hammer testing. However, when modal testing was performed using a hammer operator physically present on the floor, measured modes of vibration seemingly developed complexities indicating the presence of non-proportional damping.

Acknowledgements

The authors would like to thank the UK Access Flooring Association, PSC Freyssinet (UK) and Taywood Engineering, the research partners collaborating with the Centre for Cement and Concrete at the University of Sheffield, UK in a research project (Ref. CI 39/3/393 cc0952) funded by the 1995 Partners in Technology scheme supported by the UK government. Thanks also go to Ove Arup R&D in London. Finally, special thanks to our Ph.D. supervisor Professor Peter Waldron for his continuing support and advice.

References

[1] ANSYS user's manual, Revision 5.2: elements (Volume III). Houston, USA: ANSYS, Inc.; 1995.
[2] Brownjohn JMW, Xia P. Dynamic assessment of curved cable-stayed bridge by model updating. ASCE J Struct Eng 2000; 126(2):252–60.
[3] Post-tensioned concrete floors design handbook. Technical report 43. Slough, UK: Concrete Society; 1994.
[4] Handbook on guidelines to best practice, Volume 3—Modal testing. Cranfield, UK: UK Dynamic Testing Agency (DTA); 1993.
[5] Modal testing primer on best practice in dynamic testing. Cranfield, UK: UK Dynamic Testing Agency (DTA); 1993.
[6] Ewins DJ. Modal testing: theory, practice and application. 2nd ed. Taunton, UK: Research Studies Press Ltd. and John Wiley & Sons; 2000.
[7] Friswell MI, Mottershead JE. Finite element model updating in structural dynamics. Dordrecht, The Netherlands: Kluwer Academic Publishers; 1995.
[8] Halvorsen WG, Brown DL, 1977. Impulse technique for structural frequency response testing. A reprint from sound and vibration. Buffalo, USA: PSC Piezotronics, Inc.; November 1977. p. 8–21.
[9] Heylen W, Lammens S, Sas P. Modal testing theory and testing. Leuven, Belgium: Katholieke Universiteit; 1997.
[10] MODENT, MODESH, MODACQ, MESHGEN reference manual (Version 6). London, UK: Imperial College Analysis and Testing Software (ICATS); 1997.
[11] Methods for the experimental determination of mechanical mobility, Part 5: Measurements using impact excitation with an

exciter which is not attached to the structure. Geneva, Switzerland, ISO 7626-5.
[12] Lyndon FD, Iacovou M. Some factors affecting the dynamic modulus of elasticity of high strength concrete. Cem Concr Res 1995;25(6):1246–56.
[13] Maia NMM, Silva JMM, He J, Lieven NAJ, Lin RM, Skingle GW, et al. Theoretical and experimental modal analysis. Taunton, UK: Research Studies Press Ltd. and John Wiley & Sons; 1997.
[14] McConnell KG. Vibration testing theory and practice. New York, USA: John Wiley and Sons; 1995.
[15] A finite element dynamics primer. Glasgow, UK: NAFEMS; 1992.
[16] Neville AM. Properties of concrete. 4th ed. Harlow, UK: Longman; 1995.
[17] Price B. Stronger, bigger, better. Concrete 1996;(January/February):28–9.